Available online at www.sciencedirect.com
SCIENCE DIRECT®
Journal of Nuclear Materials 350 (2006) 113–121
journal of nuclear materials
www.elsevier.com/locate/jnucmat

Mechanical behavior of δ-phase Pu–Ga alloys. Part I: Constitutive model

M.G. Stout, G.C. Kaschner *, S.S. Hecker

Materials Science and Technology Division, Los Alamos National Laboratory, MS G756, Los Alamos, NM 87545, USA

Received 5 July 2005; accepted 24 October 2005

Abstract

We developed a constitutive model, based on the mechanical threshold strength (MTS) model reported by Follansbee and Kocks [P.S. Follansbee, U.F. Kocks, Acta Metall. 36 (1988) 81], to predict the stress/strain behavior of face-centered cubic (fcc) δ-stabilized plutonium–gallium (Pu–Ga) alloys. Input to the model is derived from our previous work on other fcc metals and published test data for Pu–Ga alloys. The model accounts for the effects of temperature, strain rate, grain size, and alloy content on the constitutive behavior. In Part I, we describe the development of the model and present all the pertinent equations and parameters. In Part II, we validate the model against existing literature data and demonstrate how the model is used to quantify the effects of test condition, grain size, alloy content, and impurity levels.

1. Introduction

Plutonium exhibits six distinct crystal structures between absolute zero and its melting point with very large volume changes accompanying several of the phase changes. At room temperature and below, it is in the brittle, low-symmetry monoclinic α-phase. At 315 °C, it takes on the highly symmetric δ-phase face-centered cubic (fcc) structure. The addition of 1–9 at.% gallium or aluminum retains the δ-phase (in a metastable condition) – which exhibits low strength and high ductility, similar to commercially pure aluminum – to room temperature [2]. A better understanding of the mechanical properties of Pu–Ga alloys is important to keep the US nuclear-weapons stockpile safe, secure, and reliable, especially in light of the decision to stop underground nuclear testing [3]. Programs that focus on the safe storage and disposition of excess weapons plutonium in the United States and Russia also need such properties.

Robbins recently reviewed the mechanical properties of δ-phase Pu–1 wt% Ga (3.35 at.%) alloys [4]. We examined the mechanical properties of Pu–Ga alloys for a range of gallium concentrations and purities, tested over a large range of temperatures and strain rates as shown in Table 1 [5–10]. As noted by Robbins and previously shown by the authors [11], the mechanical properties vary substantially. As expected, the microstructures of the samples tested in these studies also varied

DOI of original article: 10.1016/j.jnucmat.2005.10.016
* Corresponding author. Tel.: +1 505 606 0107; fax: +1 505 667 8021.
E-mail address: kaschner@lanl.gov (G.C. Kaschner).

0022-3115/$ - see front matter © 2005 Elsevier B.V. All rights reserved.
doi:10.1016/j.jnucmat.2005.10.017

Table 1
Test conditions and microstructures characterizing the mechanical behavior results reported in the literature

Experimental condition	Range of the variable
Temperature, °C	−60 to 558
Strain rates, s^{-1}	1.4×10^{-5}–75
Stress state	Tension and torsion
Microstructure	
Grain size, μm	$1–30\times90$
Composition	
Gallium content, wt%	0.29–1.63
Iron and nickel content, wt ppm	<30–900
Carbon concentration, wt ppm	30–310
Experimental results	
Yield stress (tension), MPa	48–125
Ultimate tensile strength, MPa	66–174

substantially, reflecting different gallium contents, impurity levels, and processing conditions. Robbins provides a very useful review of property trends for the Pu–1 wt% Ga alloy as a function of temperature, strain rate, and grain size [4]. However, to extend these trends to other Pu–Ga alloys and to isolate the individual effects of test and microstructural variables requires the development of a model based on the alloys' physical deformation mechanisms.

In Part I, we implement the physically based mechanical threshold strength (MTS) model developed by Follansbee and Kocks [1], using a few key experiments documented in the literature. In Part II, we validate that model against 50 ambient-pressure, quasi-static experiments reported in the literature and use the model to predict the effects of gallium concentration, grain size, and various impurities on the yield and ultimate strengths of δ-phase Pu–Ga alloys.

2. Mechanical threshold strength model: introduction

The MTS model incorporates an accurate representation of thermally activated deformation mechanisms based on the pioneering work of Kocks et al. [12] and Mecking and Kocks [13]. The model is appropriate for single-phase fcc metals whose dislocation glide kinetics are controlled by thermally activated dynamic recovery. We believe that this is the case for gallium-stabilized δ-phase plutonium at ambient pressure, quasi-static strain rates, and from room temperature to nearly 400 °C. Barmore and Uribe's strain-rate sensitivity data as a function of temperature [14] and Wheeler and Robbins' hot-torsion experimental saturation-stress levels [8] provide the basis for this conclusion. For creep-rate deformation, the upper temperature limit of the model's validity could be lower.

The MTS model assumes that the stress is the linear sum of three terms. The first two of these terms sum to the material's yield strength, while the third term accounts for the material's work hardening. The model is represented by the following expression:

$$\frac{\sigma}{\mu(T,\text{wt\% Ga})}=\frac{\sigma_a}{\mu(T,\text{wt\% Ga})}+S_i(\dot{\varepsilon},T)\frac{\hat{\sigma}_i(\text{wt\% Ga})}{\mu_0(\text{wt\% Ga})}+S_e(\dot{\varepsilon},T)\frac{\hat{\sigma}_e(\dot{\varepsilon},T)}{\mu_0(\text{wt\% Ga})}, \quad (1)$$

where μ is the shear modulus at the current temperature, μ_0 is the shear modulus at zero K, $S_i(\dot{\varepsilon},T)$ and $S_e(\dot{\varepsilon},T)$ are functions, σ_a is a constant, $\hat{\sigma}_i$ is a reference strength, termed the *mechanical threshold strength*, and $\hat{\sigma}_e(\dot{\varepsilon},T)$ is a reference strength that depends on the temperature and strain-rate history of plastic deformation. The mechanical threshold strength, $\hat{\sigma}_i$, is assumed to be the yield strength in the absence of thermal activation. In other words, $\hat{\sigma}_i$ represents the yield strength at zero K. Gallium content will affect the yield strength because gallium atoms are in substitutional sites in the fcc δ-phase lattice [2]. Hence, we assume that the mechanical threshold strength is also a function of gallium content. The shear modulus of δ-phase alloys is a function of temperature and gallium content. The stress σ_a is athermal and attributed to dislocation interactions with long-range barriers, such as grain boundaries. Grain-size contributions to yield strength will be included in this term of the constitutive model.

Each of these terms must be evaluated, based on the available literature data, to construct the MTS constitutive model for the Pu–Ga alloy system. This model is used to assess the individual contributions of strain rate, temperature, and gallium content to the yield strength and to work hardening. Once these effects are included, then the effects of microstructure, such as grain size and impurities, can be isolated.

3. Mechanical threshold strength model: development

We review the procedure used to determine the coefficients for the MTS model and discuss the modi-

fications required to make it applicable to Pu–Ga alloys with different grain sizes and compositions.

3.1. Shear modulus as a function of temperature and gallium content

The shear modulus as a function of temperature and alloy composition is a key input parameter for the MTS model because it affects the line energy of dislocations that, in turn, influences the dynamics of dislocation glide. We used the shear modulus data, determined by ultrasonic methods, reported for Pu–Ga alloys by Taylor et al. [15] for low temperatures, down to 20 K, and from Harbur [16] and Migliori et al. [17] for room and elevated temperatures. Taylor, Linford, and Dean's data for Pu–1.0 wt% Ga and Pu–1.8 wt% Ga alloys annealed at 470 °C for one week, see Fig. 1, show a smooth temperature dependence with errors less than ±0.1%. Harbur's shear modulus data for well homogenized Pu–0.5 wt% Ga and Pu–1.0 wt% Ga at temperatures of 300–625 K are also shown in Fig. 1. Recently, Migliori et al. [17] have made the most accurate measurements to date using a resonant-ultrasound technique. They studied Pu – 0.68, 0.97, and 1.365 wt% alloys between 273 K and 355 K. The data from these three independent sources are reasonably consistent and cover the temperature range, 20–625 K, for the Pu–Ga system.

The expression $\mu = \mu_0 - C/(\exp(T_{\text{ref.}}/T) - 1)$ with $T_{\text{ref.}} = 273$ K and $C = 5.27 \times 10^3$ fits the temperature dependence of the shear modulus quite well. The data shown in Fig. 1 indicate a shift in the value of the shear modulus at absolute-zero temperature, μ_0, but no change in the temperature dependence with gallium content. We used a linear equation to specify the compositional dependency of the shear modulus at zero K:

$$\mu_0 = 1.7366 \times 10^4 + 2634 \times (\text{wt\% Ga}). \tag{2}$$

Eq. (2) combined with the relation

$$\mu = \mu_0 - \frac{5.27 \times 10^3}{(\exp(273/T) - 1)} \tag{3}$$

describe both the temperature and gallium compositional dependency of the shear modulus. Fig. 2 shows that these functions fit the experimental data well.

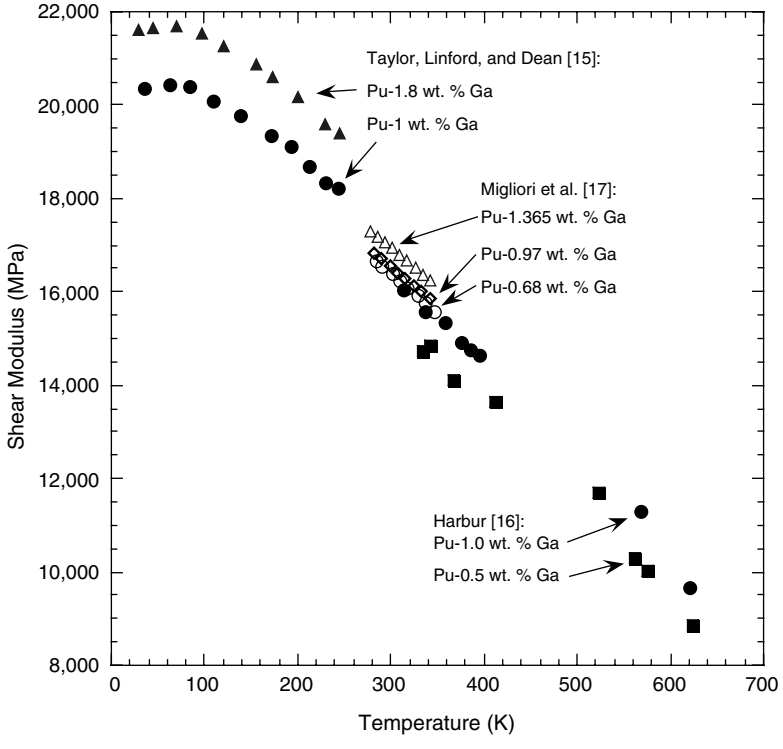

Fig. 1. Shear modulus of Pu – 0.5, 0.68, 0.97, 1.0, 1.365 and 1.8 wt% Ga alloys as a function of temperature (Pu–1 wt% Ga is equivalent to Pu–3.35 at.% Ga). Data are from Taylor et al. [15], Harbur [16], and Migliori et al. [17].

3.2. Grain-size effects

Grain-size effects must be included in the MTS model for Pu–Ga alloys because typical processing methods can yield a wide range of grain sizes. Wheeler et al. [9] found the grain-size dependency of the yield strength, in both tension and compression, to be moderate and well described by the classical Hall–Petch relation, $\sigma_y = \sigma_0 + \frac{\kappa}{\sqrt{d}}$, where σ_0 and κ are constants and d is the grain size. They determined values for σ_0 and κ of 66.8 MPa and 82.7 MPa $\mu m^{1/2}$, respectively. This value for κ compares to a value of 70 for aluminum, 120 for copper, 220 for nickel, and 70 for silver [18]. Wheeler, Thayer, and Robbins determined this relationship using a Pu–1 wt% Ga alloy with grain sizes of 1, 4, and 7 μm.

The literature contains little information about the grain-size dependency of work hardening in Pu–Ga alloys. We, therefore, examined the grain-size dependency of yield strength and work hardening in two other fcc metals, an Al–6% Ni alloy [19] and Monel 400 [20], a nickel base alloy with 32% Cu, 2.1% Fe, and 1.0% Mn. Grain-size effects were studied over a range of grain sizes from 1.2 μm to 6.25 μm and 9.5 μm to 202 μm, for the Al–6% Ni and Monel 400 respectively. In both cases, the grain size affected the yield strength but did not appear to influence the hardening behavior. In other words, the grain-size effect manifested itself as a vertical shift in the stress/strain curves, with finer grain sizes exhibiting higher yield strengths.

Based on these results, we incorporated grain-size effects as an additive term to the yield strength in Pu–Ga alloys. We defined a reference grain size and then employed the Hall–Petch relation with the parameters determined by Wheeler, Thayer, and Robbins to account for different grain sizes. In Eq. (1), this increment of yield strength was added to the term σ_a, which will be given a value sufficient to assure that the sum is a positive number. Expressing this algebraically yields

$$\Delta\sigma_{gs} = \left(\sigma_0 + \kappa\frac{1}{\sqrt{d}}\right) - \left(\sigma_0 + \kappa\frac{1}{\sqrt{d_0}}\right). \tag{4}$$

If we combine the terms in Eq. (4) and add $\Delta\sigma_{gs}$ to σ_a, Eq. (1) becomes

$$\frac{\sigma}{\mu} = \frac{1}{\mu}\left(\sigma_a + \kappa\left(\frac{\sqrt{d_0}-\sqrt{d}}{\sqrt{d_0\cdot d}}\right)\right) + S_i(\dot{\varepsilon},T)\frac{\hat{\sigma}_i}{\mu_0} + S_e(\dot{\varepsilon},T)\frac{\hat{\sigma}_e}{\mu_0}, \tag{5}$$

where $\kappa = 82.73$ MPa $\mu m^{1/2}$, d_0 is the reference grain size, and d is actual grain size in μm. The mean grain size of the materials studied in the literature was 20 μm. We chose this value for a reference grain size and set $\sigma_a = 10$ MPa, which is typical for fcc metals. Assuming grain size does not affect the hardening as was the case for the Al–6% Ni and Monel 400, no grain-size term was incorporated into the third part of Eq. (5).

3.3. Influence of the mechanical threshold strength on yield strength

Follansbee and Kocks [1] specified the function $S_i(\dot{\varepsilon},T)$ as

$$S_i(\dot{\varepsilon},T) = \left[1 - \left(\frac{kT}{\mu b^3 g_{0i}}\ln\left(\frac{\dot{\varepsilon}_{0i}}{\dot{\varepsilon}}\right)\right)^{1/q_i}\right]^{1/p_i}. \tag{6}$$

In Eq. (6), k is Boltzmann's constant ($k = 1.38^{-23}$ J/K), b is the Burger's vector ($b = 3.28\times10^{-10}$ m), $\dot{\varepsilon}_{0i}$ is a reference strain rate, typically $\dot{\varepsilon}_{0i} = 10^7\ s^{-1}$, q_i and p_i are constants routinely taken to be 3/2 and 1/2 respectively, μ is the shear modulus based on Eqs. (2) and (3), T is the temperature, $\dot{\varepsilon}$ is the strain rate, and finally g_{0i} is a constant that must be determined. This expression has the form of an Arrhenius relation appropriate for thermally activated processes.

For the moment, we will ignore the material's work hardening and consider only the first two terms in Eq. (5):

$$\frac{\sigma_{ys}}{\mu} = \frac{1}{\mu}\left(\sigma_a + \kappa\left(\frac{\sqrt{d_0}-\sqrt{d}}{\sqrt{d_0\cdot d}}\right)\right) + S_i(\dot{\varepsilon},T)\frac{\hat{\sigma}_i}{\mu_0} \tag{7}$$

or, substituting for $S_i(\dot{\varepsilon},T)$,

$$\frac{\sigma_{ys}}{\mu} = \frac{1}{\mu}\left(\sigma_a + \kappa\left(\frac{\sqrt{d_0}-\sqrt{d}}{\sqrt{d_0\cdot d}}\right)\right) + \left[1 - \left(\frac{kT}{\mu b^3 g_{0i}}\ln\left(\frac{\dot{\varepsilon}_{0i}}{\dot{\varepsilon}}\right)\right)^{1/q_i}\right]^{1/p_i}\frac{\hat{\sigma}_i}{\mu_0}. \tag{8}$$

We linearize Eq. (8) in order to solve for $\hat{\sigma}_i$ and g_{0i} explicitly from yield-strength data:

$$\left[\left(\sigma_{ys} - \sigma_a - \kappa\left(\frac{\sqrt{d_0}-\sqrt{d}}{\sqrt{d_0 d}}\right)\right)\Big/\mu\right]^{p_i} = \left(\frac{\hat{\sigma}_i}{\mu_0}\right)^{p_i} - \left(\frac{\hat{\sigma}_i}{\mu_0}\right)^{p_i}\left(\frac{1}{g_{0i}}\right)^{1/q_i}\cdot\left(\frac{kT}{\mu b^3}\cdot\ln\left(\frac{\dot{\varepsilon}_{0i}}{\dot{\varepsilon}}\right)\right)^{1/q_i}. \tag{9}$$

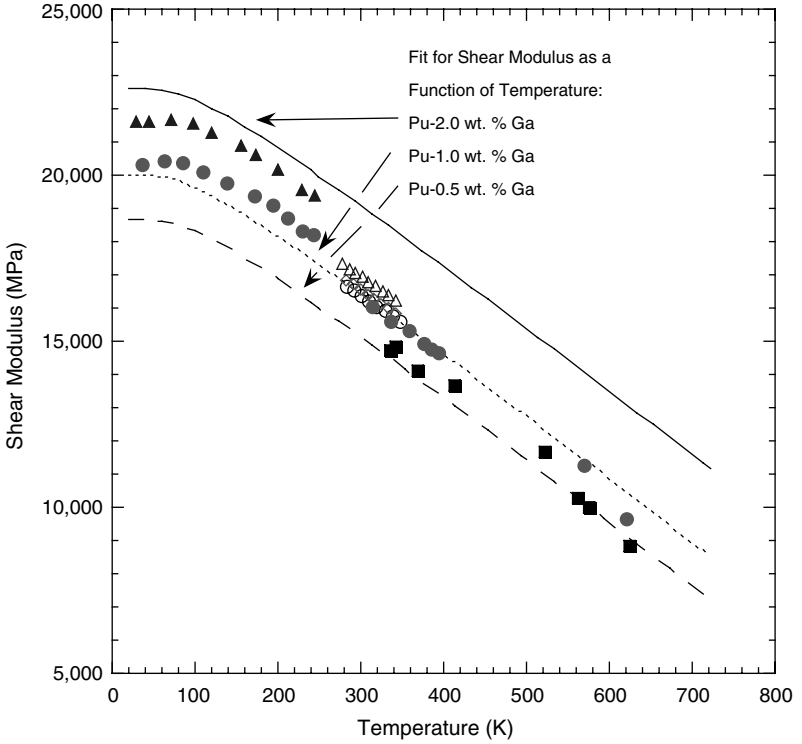

Fig. 2. Prediction of shear modulus as a function of temperature for Pu – 0.5, 1.0, and 2.0 wt% Ga compared to the experimental results shown in Fig. 1.

Beitscher [5], Hecker and Morgan [6], and Miller and White [7] published yield strengths for Pu–1 wt% Ga. We used their data substituting the appropriate grain size, temperature, strain rate, and assuming a reference grain size of $d_0 = 20$ μm to solve for $\hat{\sigma}_i$ and g_{0i}. On this basis, we determined that $g_{0i} = 0.7098$ and that $\hat{\sigma}_i = 235.5$ MPa for the Pu–1 wt% Ga alloy in question.

The values of the coefficients p_i, q_i, and $\dot{\varepsilon}_{0i}$ were based on those determined for similar materials evaluated with the MTS model. Using a value of $g_{0i} = 0.7098$, we calculated the values of $\hat{\sigma}_i$ associated with a particular yield strength and Pu–Ga composition. These results, plotted in Fig. 3, demonstrate that the mechanical threshold strength increases with increasing gallium content. We fit this dependency with a second order polynomial, $\hat{\sigma}_i = 197.49 - 30.424 \times (\text{wt\% Ga}) + 68.438 \times (\text{wt\% Ga})^2$ and found the degree of error is no worse than the scatter in the experimental data.

3.4. Work hardening behavior

Work hardening describes the increase in flow stress with increasing deformation before saturation is reached or the specimen reaches its ultimate strength in tension and begins to deform non-uniformly; that is, it necks. In fcc metals, work hardening is caused by dislocation multiplication, dislocation–solute interactions, and dislocation–dislocation interactions. Saturation occurs as dislocation hardening and dynamic recovery evenly balance one another.

3.4.1. Governing equations

The work hardening law, the last term in Eq. (1), was formulated by Follansbee and Kocks [1] in a manner very similar to the yield term. They used a reference strength value, and then discounted the reference strength as a function of the extent of thermal activation. In this case, the reference strength is not a constant but a function of the evolution of plastic deformation. Thermal activation is accounted for by the term $S_e(\dot{\varepsilon}, T)$ in Eq. (1):

$$S_e(\dot{\varepsilon}, T) = \left[1 - \left(\frac{kT}{\mu b^3 g_{0e}} \ln\left(\frac{\dot{\varepsilon}_{0e}}{\dot{\varepsilon}}\right)\right)^{1/q_e}\right]^{1/p_e} \tag{10}$$

in which we assign $p_e = 2/3$, $q_e = 1$, $\dot{\varepsilon}_{0e} = 10^7\ \text{s}^{-1}$, and $g_{0e} = 1.6$. These values are typical for other

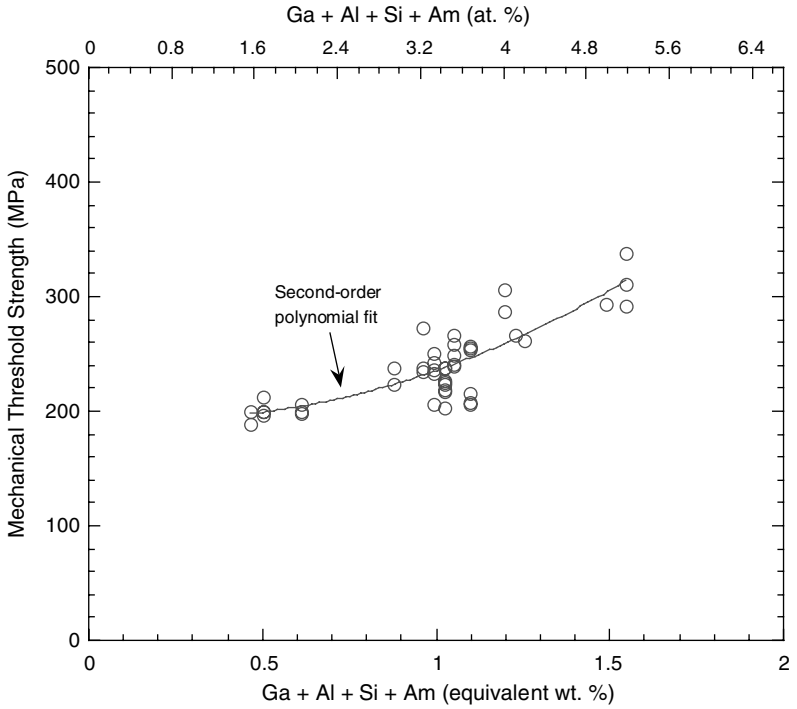

Fig. 3. The influence of gallium content on the value of the mechanical threshold strength, $\hat{\sigma}_i$. The dependency was fitted with a second order polynomial: $\hat{\sigma}_i = 197.49 - 30.424x + 68.438x^2$, where $x = \text{Ga} + \text{Al} + \text{Si} + \text{Am}$ equivalent wt%. The elements Al, Si, and Am all promote retention of the fcc δ-phase and are assumed to have the same effect as Ga on an at.% basis [2].

fcc metals. The other terms in Eq. (10) have their conventional definition.

The key to the hardening law is the definition of the reference flow stress, $\hat{\sigma}_e$. Because $\hat{\sigma}_e$ evolves for each increment of plastic strain as a function of the temperature and strain rate of that particular straining increment, it must be expressed in differential form:

$$\frac{\mathrm{d}\hat{\sigma}_e}{\mathrm{d}\varepsilon} = \Theta_0 \left[1 - \frac{\hat{\sigma}_\varepsilon}{\hat{\sigma}_{es}(\dot{\varepsilon}, T)}\right]^{\alpha}. \tag{11}$$

In Eq. (11), the initial slope of the stress/strain curve, Θ_0, and a saturation stress, $\hat{\sigma}_{es}$, define the hardening law. By defining the law in this fashion, we are assuming that a constant stress level is approached at large strain. Theoretically, Θ_0 should be a material dependent constant and should not be a function of strain rate or temperature [21]. Accordingly, based on Beitscher's data [5] we take $\Theta_0 = 2000$ MPa.

The saturation stress in Eq. (11) is that appropriate for the instantaneous temperature and strain rate of that straining increment. This saturation stress includes thermal activation. To remove the dependency on thermal activation we must reference $\hat{\sigma}_{es}$ to the saturation stress at zero K, $\hat{\sigma}_{0es}$, which is a constant. We accomplished this in the same manner as Follansbee and Kocks, through a logarithmic relationship:

$$\ln\left(\frac{\dot{\varepsilon}}{\dot{\varepsilon}_{0es}}\right) = \frac{\mu b^3 g_{0es}}{kT} \ln\left(\frac{\hat{\sigma}_{es}}{\hat{\sigma}_{0es}}\right). \tag{12}$$

In Eq. (12), the physical coefficients have their usual meaning and $\dot{\varepsilon}_{0es} = 10^7\ \mathrm{s}^{-1}$. The parameters g_{0es} and $\hat{\sigma}_{0es}$ must be found empirically by fitting hardening curves that were taken at a number of temperatures and strain rates. Some data must extend to strains greater than those of the classic tensile test for the evaluation of g_{0es} and $\hat{\sigma}_{0es}$ to be accurate. Compression or torsion tests provide this type of data.

Wheeler and Robbins [8] conducted large-strain torsion experiments on a high purity, <300 ppm of metallic impurities, Pu–1 wt% Ga alloy using a long, solid-cylinder torsion geometry. Their cylinders were twisted as many as 400 revolutions, to shear strains greater than 17, at a constant shear-strain rate of $\dot{\gamma} = 4.17 \times 10^{-2}\ \mathrm{s}^{-1}$ on the surface of the specimen. They conducted experiments at and above room temperature in 50 °C increments up to

450 °C, using a vacuum chamber and a resistance furnace.

We calculated the shear-stress/shear-strain curves that result from the torque/angle data, based on values of work hardening, Hecker and Morgan [6], and strain-rate sensitivity, Hecker and Morgan [6] and Barmore and Uribe [14], found in the literature for a Pu–1 wt% Ga alloy. We describe this procedure in detail [20].

Fig. 4 shows these stress/strain results for the high-purity metal, combined with a treatment of the data for which we assumed no strain-rate sensitivity or work hardening. As expected, at high temperatures the two solutions converge because the constitutive behavior of the Pu–1 wt% Ga approaches perfectly plastic. In Fig. 4, we plot 'effective stress' versus 'effective strain,' using the von Mises definition of effective stress and effective strain to compare torsion and uniaxial tension experiments. By combining Wheeler and Robbins' torsion results with Hecker and Morgan's, and Beitscher's tensile data, we established a dataset for evaluating the hardening behavior in the MTS law.

3.4.2. Fitting the hardening law

The descriptions of work hardening given by Eqs. (11) and (12) remain to be fit, by specifying g_{0es}, $\hat{\sigma}_{0es}$, and α. In Eq. (11), the initial slope, Θ_0, and saturation stress, $\hat{\sigma}_{es}$, of the hardening curve are known. Only the parameter α needs to be determined. The term α affects the degree of 'bow' in the stress/strain curve between the initial slope and the saturation stress. For the Pu–1 wt% Ga we found that $\alpha = 2$ best fits the literature data.

The two terms g_{0es} and $\hat{\sigma}_{0es}$ are the most critical to fit the hardening behavior. The term g_{0es} controls the spread between the hardening curves as a function of temperature and strain rate. Too large a value of g_{0es} produces insufficient temperature or strain-rate sensitivity, whereas too low a value results in excessive sensitivity. The constant $\hat{\sigma}_{0es}$ controls the saturation-stress level of the hardening curves. If predictions from the model lie below the torsion data, the value of $\hat{\sigma}_{0es}$ must be increased and visa versa.

The experimental data represented by the solid lines and the predictions from our full model represented by the symbols are compared in Fig. 5.

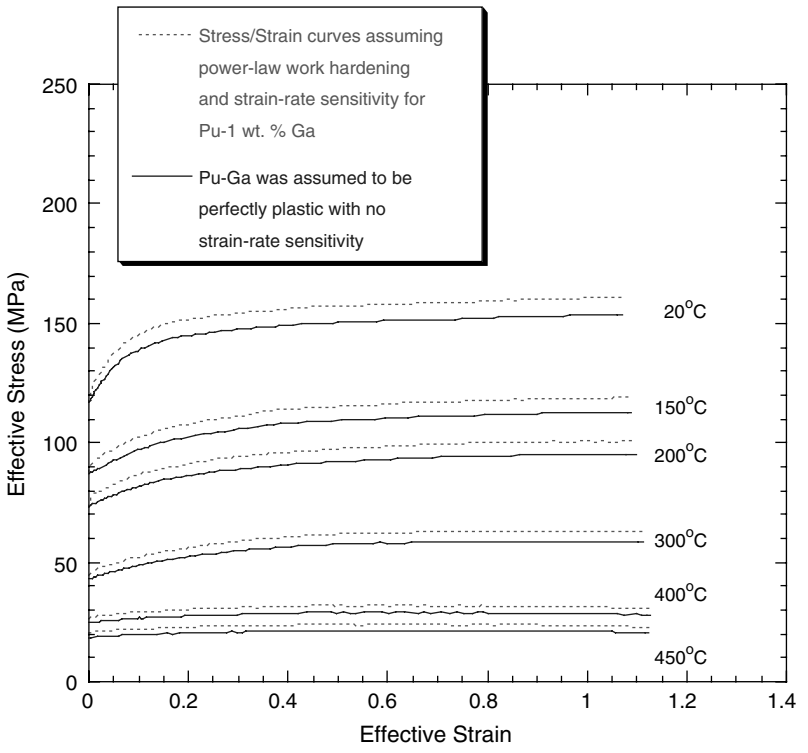

Fig. 4. The upper and lower bounds effective stress/strain curves we calculated from Wheeler and Robbins' [8] torque/angle data for torsion experiments on a high purity Pu–1 wt% Ga alloy at different temperatures (irregularities in the curves are a result of digitization).

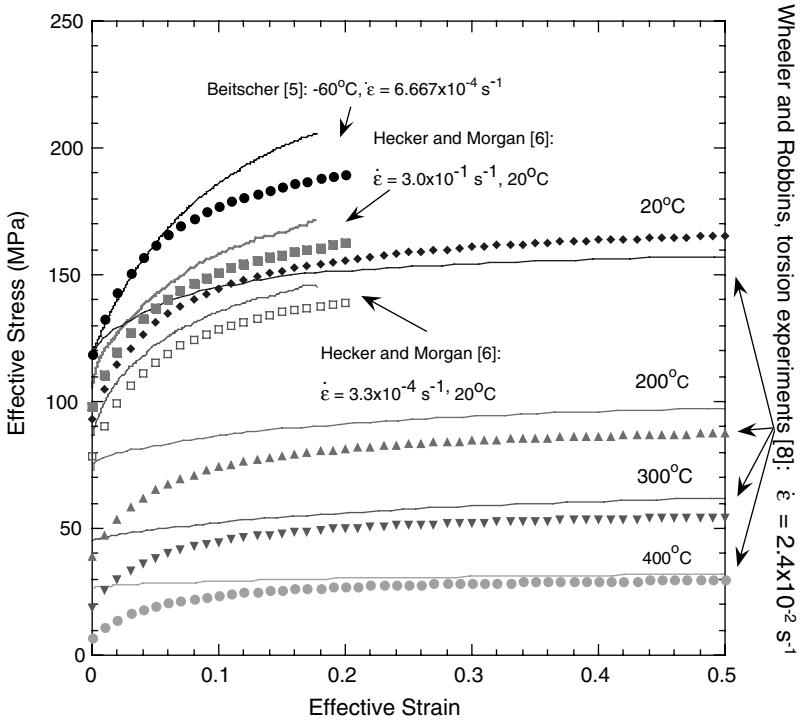

Fig. 5. The experimental stress/strain data used to fit the work-hardening law, solid lines, and the hardening behavior predicted by the MTS law for $\alpha = 2$, $g_{0es} = 3.6$, and $\hat{\sigma}_{0es} = 115$ MPa.

The best agreement between model and simulation was obtained for values of $g_{0es} = 3.6$ and $\hat{\sigma}_{0es} = 115$ MPa.

The yield strengths predicted by the MTS model deviate from Hecker and Morgan's data, but the hardening behavior follows their data well. We optimized the MTS model's fit of yield behavior independent of these data, and the difference between the model's prediction and Hecker and Morgan's experiments reflect expected deviations between experiment and theory. We will consider the severity of these deviations in Part II, in which we discuss model validation.

It is apparent from Fig. 5 that the saturation stresses at large strains are matched well as a function of temperature. However, our model does not fit the torsion yield response accurately. These deviations likely result from our inability to resolve yield strains of <0.05 on the plots published by Wheeler and Robbins. In addition, because of the large stress and strain gradients across the radius of the cylinder, the surface of the torsion sample yields while the center remains elastic.

Also, we were unable to fit the hardening curve of Beitscher at −60 °C. All of our other fits of tensile-test hardening behavior at different strain rates and higher temperatures are accurate, and this leads us to suspect the applicability of the −60 °C experimental result. As shown by Hecker et al. [2], it is quite possible to induce transformation of the retained δ-phase to the α-phase at low temperatures. If the $\delta \rightarrow \alpha$ transformation occurred, it would have increased the work hardening of the −60 °C test over the MTS model's prediction, consistent with the reported experimental results.

4. Discussion and conclusions

We constructed and fitted the MTS model to predict the yield and flow stress behavior for single-phase δ-stabilized Pu–Ga alloys as a function of strain rate and temperature. Our model accounts for variations in gallium content and grain size. The full description of the model and all of its coefficients are tabulated in Appendix A. The model is based only on published quasi-static, ambient-pressure data.

In the accompanying Part II paper, we validate the model by considering all existing literature Pu–Ga alloy data. The validation compares the mod-

el's prediction against published yield and ultimate tensile strengths. We also use the model to assess the significance of different compositional and microstructural variables. For example, we ascertain the strengthening effects of the gallium alloying additions, the significance of iron and nickel or carbon content, and the influence of grain size on strength.

Appendix A. Equations used for the MTS model fit to Pu–Ga

- $$\frac{\sigma}{\mu} = \frac{1}{\mu}\left(\sigma_a + \kappa\left(\frac{\sqrt{d_0} - \sqrt{d}}{\sqrt{d_0 d}}\right)\right) + S_i(\dot{\varepsilon}, T)\frac{\hat{\sigma}_i}{\mu_0} + S_\varepsilon(\dot{\varepsilon}, T)\frac{\hat{\sigma}_\varepsilon}{\mu_0},$$

  where $\sigma_a = 10$ MPa; $d_0 = 20$ μm; $d =$ alloys grain size in μm; $\kappa = 82.73$ MPa $\mu m^{1/2}$.

- $$\mu = \mu_0 - \frac{5270 \text{ MPa}}{\exp\left(\frac{273 \text{ K}}{T}\right) - 1},$$

  where $\mu_0 = 2 \times 10^4$ MPa; $\mu_0 = 17366 + 2634 \times$ (wt% Ga).

- $$S_i(\dot{\varepsilon}, T) = \left[1 - \left(\frac{kT}{\mu b^3 g_{0i}} \ln\left(\frac{\dot{\varepsilon}_{0i}}{\dot{\varepsilon}}\right)\right)^{1/q_i}\right]^{1/p_i},$$

  where $\frac{k}{b^3} = 0.3911$ MPa/K; $k = 1.38 \times 10^{-23}$ J/K; $b = 3.28 \times 10^{-10}$ m; $\dot{\varepsilon}_{0i} = 1 \times 10^7$ s^{-1}; $g_{0i} = 0.7098$; $q_i = 1.5$, $p_i = 0.5$; $\frac{\hat{\sigma}_i}{\mu_0} = 0.012025$ (or $\hat{\sigma}_i = 240.5$ MPa); $\hat{\sigma}_i = 197.49 - 30.424 \times (\text{wt\% Ga}) + 68.438 \times (\text{wt\% Ga})^2$.

- $$S_e(\dot{\varepsilon}, T) = \left[1 - \left(\frac{kT}{\mu b^3 g_{0e}} \ln\left(\frac{\dot{\varepsilon}_{0e}}{\dot{\varepsilon}}\right)\right)^{1/q_i}\right]^{1/p_i},$$

  where $\dot{\varepsilon}_{0e} = 1 \times 10^7$ s^{-1}; $g_{0e} = 1.6$; $q_e = 1$; $p_e = 2/3$.

- $$\frac{d\hat{\sigma}_e}{d\varepsilon} = \Theta_0\left[1 - \frac{\hat{\sigma}_\varepsilon}{\hat{\sigma}_{es}(\dot{\varepsilon}, T)}\right]^\alpha,$$

  where $\theta_0 = 2000$ MPa, $\alpha = 2$.

- $$\ln\left(\frac{\dot{\varepsilon}}{\dot{\varepsilon}_{0es}}\right) = \frac{\mu b^3 g_{0es}}{kT} \ln\left(\frac{\hat{\sigma}_{es}}{\hat{\sigma}_{0es}}\right),$$

  where $g_{0es} = 3.6$; $\hat{\sigma}_{es0} = 115$ MPa; $\dot{\varepsilon}_{0es} = 1 \times 10^7$ s^{-1}.

The coefficients were determined based on open literature data at strain rates at and below 3.0 s^{-1}.

References

[1] P.S. Follansbee, U.F. Kocks, Acta Metall. 36 (1988) 81.
[2] S.S. Hecker, D.R. Harbur, T.G. Zocco, Prog. Mater. Sci. 49 (2004) 429.
[3] S.S. Hecker, Los Alamos Science (2000) 4.
[4] J.L. Robbins, J. Nucl. Mater. 324 (2004) 125.
[5] S. Beitscher, J. Nucl. Mater. 24 (1967) 113.
[6] S.S. Hecker, J.R. Morgan, in: H. Blank, R. Lindner (Eds.), Plutonium 1975 and Other Actinides, North-Holland, Amsterdam, 1976, p. 697.
[7] D.C. Miller, J.S. White, J. Nucl. Mater. 17 (1965) 54.
[8] A.D. Wheeler, J.L. Robbins, J. Nucl. Mater. 32 (1969) 57.
[9] A.D. Wheeler, W.L. Thayer, J.L. Robbins, in: W.A. Miner (Ed.), Plutonium 1970 and Other Actinides, Metallurgical Society of AIME, New York, 1971, p. 437.
[10] S.S. Hecker, LANL, 1999, private communication.
[11] M.G. Stout, G.C. Kaschner, S.S. Hecker, LANL, 2002, LA-994458-PR.
[12] U.F. Kocks, A.S. Argon, M.F. Ashby, Thermodynamics and Kinetics of Slip, Pergamon, Oxford, New York, 1975.
[13] H. Mecking, U.F. Kocks, Acta Metall. 29 (1981) 1865.
[14] W.L. Barmore, F.S. Uribe, in: W.A. Miner (Ed.), Plutonium 1970 and Other Actinides, Metallurgical Society of AIME, New York, 1971, p. 414.
[15] J.C. Taylor, P.F.T. Linford, D.J. Dean, J. Inst. Metals 96 (1968) 178.
[16] D.R. Harbur, LANL, 1999, private communication.
[17] A. Migliori, F. Freibert, J.C. Lashley, A.C. Lawson, J.P. Baiardo, D.A. Miller, J. Supercond.: Incorpor. Novel Magn. 15 (2002) 499.
[18] E.O. Hall, in: Yield Point Phenomena in Metals and Alloys, Plenum, New York, 1970, p. 296.
[19] D.J. Lloyd, Metal Sci. 14 (1980) 193.
[20] G.T. Gray III, S.R. Chen, K.S. Vecchio, Metall. Trans. A 30A (1999) 1235.
[21] U.F. Kocks, H. Mecking, Prog. Mater. Sci. 48 (2003) 171.